

Validation of the SCEC Broadband Platform V14.3 Simulation Methods Using Pseudospectral Acceleration Data

by Douglas S. Dreger, Gregory C. Beroza, Steven M. Day, Christine A. Goulet, Thomas H. Jordan, Paul A. Spudich, and Jonathan P. Stewart

Online Material: Figures showing bias of PSA between data and simulations and between GMPEs and simulations for validation events and scenarios.

INTRODUCTION

This article summarizes the evaluation of ground-motion simulation methods implemented on the Southern California Earthquake Center (SCEC) Broadband Platform (BBP), version 14.3 (as of March 2014). A seven-member panel, the authorship of this article, was formed to evaluate those methods for the prediction of pseudospectral accelerations (PSAs) of ground motion. The panel's mandate was to evaluate the methods using tools developed through the validation exercise (Goulet *et al.*, 2015) and to define validation metrics for the assessment of the methods' performance. This article summarizes the evaluation process and conclusions from the panel. The five broadband, finite-source simulation methods on the BBP include two deterministic approaches herein referred to as CSM (Anderson, 2015) and UCSB (Crempien and Archuleta, 2015); a band-limited stochastic white noise method called EXSIM (Atkinson and Assatourians, 2015); and two hybrid approaches, referred to as G&P (Graves and Pitarka, 2015) and SDSU (Olsen and Takedatsu, 2015), which utilize a deterministic Green's function approach for periods longer than 1 s and stochastic methods for periods shorter than 1 s.

Two acceptance tests were defined to validate the broadband finite-source ground-motion simulation methods (Goulet *et al.*, 2015). Part A compared observed and simulated PSAs for periods from 0.01 to 10 s for 12 moderate-to-large earthquakes located in California, Japan, and the eastern United States. Part B compared the median simulated PSAs with published Next Generation Attenuation-West 1 (NGA-West 1) (Abrahamson and Silva, 2008; Boore and Atkinson, 2008; Campbell and Bozorgnia, 2008; Chiou and Youngs, 2008) ground-motion prediction equations (GMPEs) for specific magnitude and distance cases, using a pass-fail criterion based on a defined acceptable range around the spectral shape of the GMPEs. For the initial part A

and part B validation exercises during the summer of 2013, the software for the five methods was locked in at version 13.6 (v13.6; see Maechling *et al.*, 2015). In the spring of 2014, additional moderate events were considered for the part A validation, and additional magnitude and distance cases were considered for the part B validation, for the software locked in at version 14.3 (v14.3). Several of the simulation procedures, specifically UCSB and SDSU, changed significantly between v13.6 and v14.3. The CSM code was not submitted in time for the v14.3 evaluation, and its detailed performance is not addressed in this article.

As described in Goulet *et al.* (2015) and Maechling *et al.* (2015), the BBP generates a variety of products, including three-component acceleration time series. A series of postprocessing codes were developed to provide individual component PSAs and average median horizontal-component PSA (referred to as RotD50; Boore, 2010) for oscillator periods ranging from 0.01 to 10 s, as well as median PSA values computed using the NGA-West 1 GMPEs. The BBP was also configured to provide statistical analysis of simulation results relative to recordings (part A) and GMPEs (part B), as described further in the sections below.

As part of our evaluation, we reviewed documentation provided by each of the developers, which included the technical basis behind the methods and the developer's self-assessments regarding the extrapolation capabilities (in terms of magnitude and distance ranges) of their methods. Two workshops were held in which methods and results were presented, and the panel was given the opportunity to question the developers and to have detailed technical discussions. A SCEC report (Dreger *et al.*, 2013) describes the results of this review for BBP v13.6. This article summarizes that work and presents results for the more recent BBP 14.3 validation.

PART A EVALUATION METRICS AND VALIDATION RESULTS

The part A validation involved the comparison of simulated and observed PSAs for 12 earthquake events. As described

further in [Goulet *et al.* \(2015\)](#), 40 stations were selected for each event that provided good azimuthal and site–source distance coverage. RotD50 PSA was computed from the two horizontal components for 63 discrete periods ranging from 0.01 to 10 s. For each method and for each validation event, 50 realizations of the slip and rupture kinematics were simulated.

The basis for the data-to-simulation comparison was principally in terms of residuals of RotD50 PSAs (Ⓔ Fig. S1, available in the electronic supplement to this article). For a given period, the residual is defined as the difference between the natural logarithm of the observed PSA (data) and the simulations (model), which can be written as $\ln(\text{data}/\text{model})$. Positive residuals indicate an underprediction of the PSAs from the models, and negative residuals correspond to an overprediction. Although residuals were computed at each of the 63 periods considered, they were aggregated into four period bins (0.01–0.1 s, 0.1–1 s, 1–3 s, and > 3 s) and into four distance bins (0–5 km, 5–20 km, 20–70 km, and larger than 70 km) to facilitate the interpretation. Ⓔ Figure S1 shows the residuals for these selected bins. Because of the period grouping, there is potential for period-dependent trends in residuals yielding a mean of zero in a given bin. For this reason, our interpretations are based not on within-bin means, but instead upon a combined goodness-of-fit (CGOF) parameter, taken as the equally weighted sum of the absolute value of the mean residuals and the mean of the absolute value of the residuals:

$$\text{CGOF} = \frac{1}{2} \langle |\ln(\text{data}/\text{model})| \rangle + \frac{1}{2} \langle |\ln(\text{data}/\text{model})| \rangle, \quad (1)$$

in which $\langle \rangle$ denotes computation of the mean and $||$ the absolute value.

For each of the 12 validation earthquakes, residuals were computed from the 50 source realizations and selected stations (up to 40 if available). Because of the large number of residuals, nonzero means, or nonzero CGOF, can be interpreted as bias. Optimal bias is zero. We based our evaluations on bias expressed as CGOF values for residuals binned according to the aforementioned period and distance ranges using rules defined in the following section. Accordingly, CGOF values for an individual bin are based on all source realizations, observations (data) within the applicable distance range, and residuals within the applicable period range.

We identified three ways of interpreting the CGOF results. The first was to apply reasonable pass/fail thresholds, described below, to the relatively simple CGOF metrics. In addition, because PSAs for a specific event can be biased high or low due to unaccounted-for aspects of the sources (such as stress drop), a second approach was used to account for such possible event bias or event terms. In this approach, CGOF is normalized with corresponding values obtained from the NGA-West 1 GMPEs. Because the GMPEs are constructed from many events, they represent a population average; and, if a given event is biased with respect to the GMPE average and also biased with respect to the simulation results, this could be indicative of a nonzero event term. Thus the normalization of the CGOF with its counterpart from a GMPE potentially adjusts for such bias,

as well as providing an indication of whether a simulation method's performance is superior to that of the GMPE. The third approach was to evaluate potential distance trends in the residuals using averaged residuals for the four distance bins. We evaluate the slope of a linear fit in residual–log distance space; if zero slope is within the 95% confidence of the mean, the simulations are providing ground motions with a distance dependence (or attenuation level) that is grossly compatible with the data. This distance test builds on previous work by [Star *et al.* \(2011\)](#). The three metrics and their evaluation are described in the subsections that follow.

CGOF Pass Thresholds for Distance and Period Ranges

Figure 1 shows CGOF values organized into columns corresponding to the four methods in BBP v14.3 (UCSB, EXSIM, G&P, and SDSU) and the average of the NGA-West 1 GMPEs. The columns are grouped into the four period bins, and the rows are grouped into the four distance bins. Each row within a distance bin shows results for one of the 12 scenario events. Following the event-specific results, regional averages are provided for California (CA), central and eastern North America (CENA), and all events, including Japan (ALL). In each cell, the CGOF value is given in natural log units.

The thresholds adopted in the BBP evaluation are subjective. A CGOF exceeding a factor of 2.0 (0.69 ln units) was judged to be a “fail” condition, whereas a CGOF less than a factor of 1.4 (0.35 ln units) was given a “pass.” To provide perspective on this choice, we note that an amplitude shift of 0.35 ln units at long period and large distance corresponds to an event magnitude shift of 0.1 units, based on the moment magnitude relationship. Moreover, the acceptance criterion for the part B validation, discussed in the next section, is, on average, a range of ± 1.46 or ± 0.38 ln units.

Many of the simulation methods produce fail conditions for the 0–5 km distance range, which results in part from a small number of observations and difficulties in fitting data at these distances (Fig. 1). Three events (Alum Rock, Landers, and Rivière-du-Loup) stand out as being problematic for all methods in different distance and period bins. As shown in Figure 2, normalizing the CGOFs from simulations with those from NGA-West 1 GMPEs indicates that some of the bias for Alum Rock and Landers is likely due to event terms, which in turn suggests that there are unaccounted-for deviations between the actual source and the average source behavior, as characterized by the simulation method source generators. The nonzero event terms indicate similar issues with the average source term in the GMPEs.

In the 5–20 and 20–70 km distance ranges, all of the tested methods perform well on average in the 0.01–0.1 s, 0.1–1.0 s, and 1–3 s period bands. The two Japanese cases show problems at periods longer than 1 s and distances greater than 70 km that are possibly caused by strong surface waves produced by the simplified and uncalibrated crustal velocity model used. At larger distances (70–200 km), all of the methods show problematic cases considering the ± 0.35 ln unit threshold, although many of the marginal cases meet the pass threshold

Combined Metric Performance Level

Within Threshold	Potential Issues	Problematic
------------------	------------------	-------------

Event (M_w , Mech.)		0.01 ≤ PSA Period Range ≤ 0.1 s					0.1 < PSA Period Range ≤ 1 s					1 < PSA Period Range ≤ 3 s					PSA > 3s					
		UCSB	EXSIM	G&P	SDSU	GMPE	UCSB	EXSIM	G&P	SDSU	GMPE	UCSB	EXSIM	G&P	SDSU	GMPE	UCSB	EXSIM	G&P	SDSU	GMPE	
R_{rup} = [0-5] km	Chino Hills (5.39, ROBL)																					
	Alum Rock (5.45, SS)		1.04	0.94	0.65	1.33		1.15	1.11	0.78	1.33		1.15	1.32	1.32	1.77		0.96	1.11	1.05	1.66	
	Whittier Narrows (5.89, REV)																					
	North Palm Springs (6.12, ROBL)	0.25	0.38	0.13	0.36	0.16	0.96	0.23	0.11	0.27	0.16	0.93	0.20	0.47	0.51	0.15	0.41	0.08	0.94	0.95	0.50	
	Tottori (6.59, SS)	0.20	1.18	0.13	0.40	0.23	1.08	0.41	0.59	0.46	0.62	1.25	0.19	0.14	0.17	0.11	1.11	0.23	0.30	0.31	0.41	
	Niigata (6.65, REV)																					
	Northridge (6.73, REV)																					
	Loma Prieta (6.94, ROBL)	0.27	0.29	0.18	0.26	0.25	0.58	0.29	0.25	0.33	0.21	0.76	0.73	0.30	0.33	0.59	0.43	0.34	0.39	0.39	0.31	
	Landers (7.22, SS)	1.16	0.73	0.91	0.92	1.05	1.58	0.28	0.55	0.45	0.69	2.04	0.61	0.58	0.53	0.94	2.25	1.13	0.45	0.44	1.17	
	Riviere-du-Loup (4.6 REV)																					
	Mineral (5.68 REV)																					
	Saguenay (5.81 REV)																					
	Average CA	0.45	0.33	0.27	0.34	0.35	0.86	0.25	0.25	0.29	0.34	1.05	0.50	0.45	0.47	0.46	1.16	0.54	0.40	0.39	0.45	
Average CENA																						
Average ALL	0.38	0.36	0.25	0.29	0.30	0.90	0.27	0.29	0.31	0.30	1.09	0.43	0.41	0.43	0.41	1.15	0.43	0.38	0.37	0.43		
R_{rup} = [5-20] km	Chino Hills (5.39, ROBL)		0.27	0.17	0.23	0.45		0.39	0.31	0.34	0.26		0.64	0.73	0.65	0.15		0.80	0.80	0.84	0.27	
	Alum Rock (5.45, SS)		0.32	0.52	0.19	0.48		0.28	0.43	0.21	0.33		0.38	0.42	0.44	0.34		0.71	0.43	0.43	0.43	
	Whittier Narrows (5.89, REV)	0.40	0.28	0.36	0.36	0.30	0.76	0.32	0.27	0.28	0.21	0.46	0.21	0.47	0.55	0.44	0.21	0.37	1.02	1.01	0.81	
	North Palm Springs (6.12, ROBL)	0.48	0.23	0.31	0.22	0.25	0.64	0.27	0.33	0.29	0.28	0.65	0.26	0.42	0.48	0.39	0.31	0.29	0.15	0.15	0.45	
	Tottori (6.59, SS)	0.39	0.47	0.36	0.31	0.60	0.44	0.21	0.40	0.23	0.23	0.60	0.47	0.21	0.27	0.25	0.22	0.54	0.37	0.25	0.24	
	Niigata (6.65, REV)	0.43	0.34	0.36	0.34	0.48	0.62	0.39	0.32	0.23	0.42	0.18	0.34	0.63	0.67	0.47	0.26	0.34	0.61	0.62	0.61	
	Northridge (6.73, REV)	0.56	0.31	0.20	0.22	0.21	0.80	0.38	0.32	0.29	0.32	0.54	0.39	0.22	0.25	0.36	0.37	0.36	0.21	0.21	0.29	
	Loma Prieta (6.94, ROBL)	0.20	0.37	0.20	0.27	0.24	0.47	0.31	0.21	0.30	0.27	0.41	0.24	0.35	0.36	0.20	0.46	0.33	0.27	0.27	0.23	
	Landers (7.22, SS)	0.73	0.43	0.45	0.48	0.33	0.65	0.32	0.27	0.28	0.33	0.53	0.43	0.41	0.44	0.22	0.44	0.41	0.85	0.85	0.42	
	Riviere-du-Loup (4.6 REV)		0.63	0.24	0.19	0.59		0.58	0.67	0.65	0.58		0.84	0.86	0.80	0.44		1.14	1.12	1.20	0.87	
	Mineral (5.68 REV)	0.74	0.46	0.43	0.66	0.71	0.66	0.20	0.27	0.68	0.36	0.92	0.20	0.05	0.23	0.32	0.57	0.28	0.03	0.25	0.19	
	Saguenay (5.81 REV)																					
	Average CA	0.31	0.26	0.26	0.22	0.27	0.68	0.29	0.22	0.23	0.23	0.50	0.27	0.32	0.35	0.26	0.39	0.44	0.30	0.29	0.26	
Average CENA	0.74	0.57	0.30	0.35	0.63	0.66	0.40	0.52	0.58	0.44	0.92	0.59	0.54	0.48	0.38	0.57	0.93	0.84	0.90	0.70		
Average ALL	0.28	0.23	0.23	0.24	0.23	0.65	0.29	0.24	0.24	0.28	0.48	0.27	0.33	0.36	0.26	0.36	0.39	0.31	0.32	0.25		
R_{rup} = [20-70] km	Chino Hills (5.39, ROBL)		0.39	0.26	0.24	0.50		0.33	0.28	0.26	0.42		0.46	0.35	0.29	0.24		0.64	0.61	0.59	0.28	
	Alum Rock (5.45, SS)		0.77	1.04	0.76	1.01		0.80	1.03	0.75	0.84		0.63	0.82	0.84	0.88		0.22	0.56	0.57	0.42	
	Whittier Narrows (5.89, REV)	0.43	0.40	0.26	0.35	0.31	1.00	0.35	0.28	0.38	0.27	0.79	0.30	0.47	0.56	0.52	0.37	0.14	0.46	0.49	0.31	
	North Palm Springs (6.12, ROBL)	0.35	0.62	0.45	0.41	0.42	0.90	0.31	0.26	0.26	0.29	0.85	0.44	0.24	0.29	0.41	0.14	0.34	0.43	0.43	0.09	
	Tottori (6.59, SS)	0.21	0.31	0.78	0.37	1.08	0.35	0.34	0.33	0.31	0.53	0.38	0.50	0.63	0.66	0.49	0.35	0.20	0.51	0.51	0.36	
	Niigata (6.65, REV)	0.36	0.31	0.38	0.24	0.48	0.39	0.29	0.43	0.33	0.33	0.52	0.52	0.99	1.01	0.67	0.92	0.40	1.11	1.11	0.72	
	Northridge (6.73, REV)	0.53	0.20	0.30	0.55	0.32	0.26	0.28	0.34	0.42	0.24	0.29	0.57	0.35	0.38	0.38	0.43	0.35	0.57	0.57	0.27	
	Loma Prieta (6.94, ROBL)	0.59	0.25	0.50	0.38	0.34	0.25	0.27	0.43	0.30	0.24	0.23	0.37	0.50	0.51	0.24	0.49	0.39	0.27	0.27	0.48	
	Landers (7.22, SS)	0.94	0.22	0.36	0.31	0.27	0.38	0.37	0.38	0.36	0.27	0.44	0.67	0.58	0.60	0.46	0.32	0.41	0.74	0.74	0.38	
	Riviere-du-Loup (4.6 REV)		0.36	0.37	0.28	0.96		0.53	0.29	0.34	0.43		0.45	0.32	0.37	0.82		0.28	0.26	0.28	0.72	
	Mineral (5.68 REV)	0.25	0.70	0.37	0.24	1.42	0.46	0.32	0.55	1.19	0.38	0.90	0.96	0.69	0.53	0.73	0.43	1.35	0.05	0.09	0.68	
	Saguenay (5.81 REV)	1.73	0.58	1.04	0.30	1.61	1.28	0.59	0.21	1.33	0.35	0.29	1.46	1.06	1.98	1.46						
	Average CA	0.44	0.27	0.40	0.38	0.40	0.54	0.32	0.42	0.39	0.36	0.38	0.44	0.45	0.49	0.44	0.33	0.27	0.49	0.49	0.25	
Average CENA	0.89	0.42	0.44	0.26	1.09	0.87	0.45	0.29	0.55	0.41	0.86	0.53	0.34	0.40	0.78	0.43	0.41	0.23	0.26	0.64		
Average ALL	0.40	0.29	0.32	0.32	0.32	0.50	0.30	0.40	0.39	0.34	0.30	0.43	0.52	0.56	0.49	0.44	0.26	0.63	0.63	0.40		
R_{rup} = [70-200 or 300] km	Chino Hills (5.39, ROBL)		0.54	0.51	0.43	0.33		0.43	0.46	0.46	0.31		0.44	0.50	0.46	0.32		0.65	0.75	0.75	0.48	
	Alum Rock (5.45, SS)		0.79	0.82	0.67	1.02		0.89	0.88	0.63	0.89		0.27	0.83	0.86	0.36		0.16	0.86	0.86	0.21	
	Whittier Narrows (5.89, REV)																					
	North Palm Springs (6.12, ROBL)	0.26	0.15	0.09	0.25	0.25	0.52	0.46	0.36	0.48	0.43	0.83	0.46	0.37	0.30	0.35						
	Tottori (6.59, SS)	0.49	0.54	0.72	0.44	0.63	0.37	0.53	0.40	0.59	0.38	0.31	0.52	0.50	0.51	0.51	0.27	0.81	0.45	0.45	0.32	
	Niigata (6.65, REV)	0.35	0.31	0.35	0.42	0.49	0.37	0.44	0.79	0.33	0.81	0.70	0.52	1.33	1.35	1.05	1.35	0.33	1.50	1.50	0.92	
	Northridge (6.73, REV)	0.30	0.28	0.31	0.17	0.18	0.31	0.32	0.40	0.34	0.40	0.27	0.86	0.43	0.44	0.56	0.03	0.56	0.31	0.31	0.18	
	Loma Prieta (6.94, ROBL)	0.24	0.61	0.41	0.54	0.45	0.63	0.64	0.58	0.76	0.73	0.94	0.88	0.74	0.72	1.19	0.66	0.49	0.33	0.33	0.79	
	Landers (7.22, SS)	0.18	0.08	0.10	0.15	0.19	0.45	0.33	0.20	0.25	0.22	0.69	0.37	0.23	0.21	0.45	0.96	0.33	0.25	0.25	0.78	
	Riviere-du-Loup (4.6 REV)		0.45	0.44	0.23	1.51		0.69	0.51	0.34	0.88		0.84	0.70	0.62	0.64		0.97	0.69	0.58	0.16	
	Mineral (5.68 REV)	0.61	0.33	0.46	0.21	1.31	1.38	0.32	0.36	0.41	1.03	1.46	0.57	0.87	0.80	0.64	0.46	1.08	0.25	0.24	0.76	
	Saguenay (5.81 REV)	2.56	0.49	1.05	0.21	1.68	3.57	0.77	1.43	0.30	1.47	2.91	0.52	1.63	0.56	0.67	0.66	0.12	0.37	0.13	0.26	
	Average CA	0.16	0.27	0.24	0.25	0.35	0.48	0.37	0.32	0.29	0.35	0.70	0.31	0.34	0.36	0.39	0.93	0.39	0.35	0.35	0.54	
Average CENA	1.71	0.41	0.62	0.20	1.52	2.62	0.60	0.85	0.34	1.18	2.13	0.60	1.12	0.68	0.60	0.48	0.98	0.27	0.23	0.68		
Average ALL	0.50	0.34	0.38	0.29	0.52	0.82	0.34	0.37	0.36	0.44	0.70	0.34	0.50	0.51	0.42	0.58	0.51	0.69	0.69	0.42		

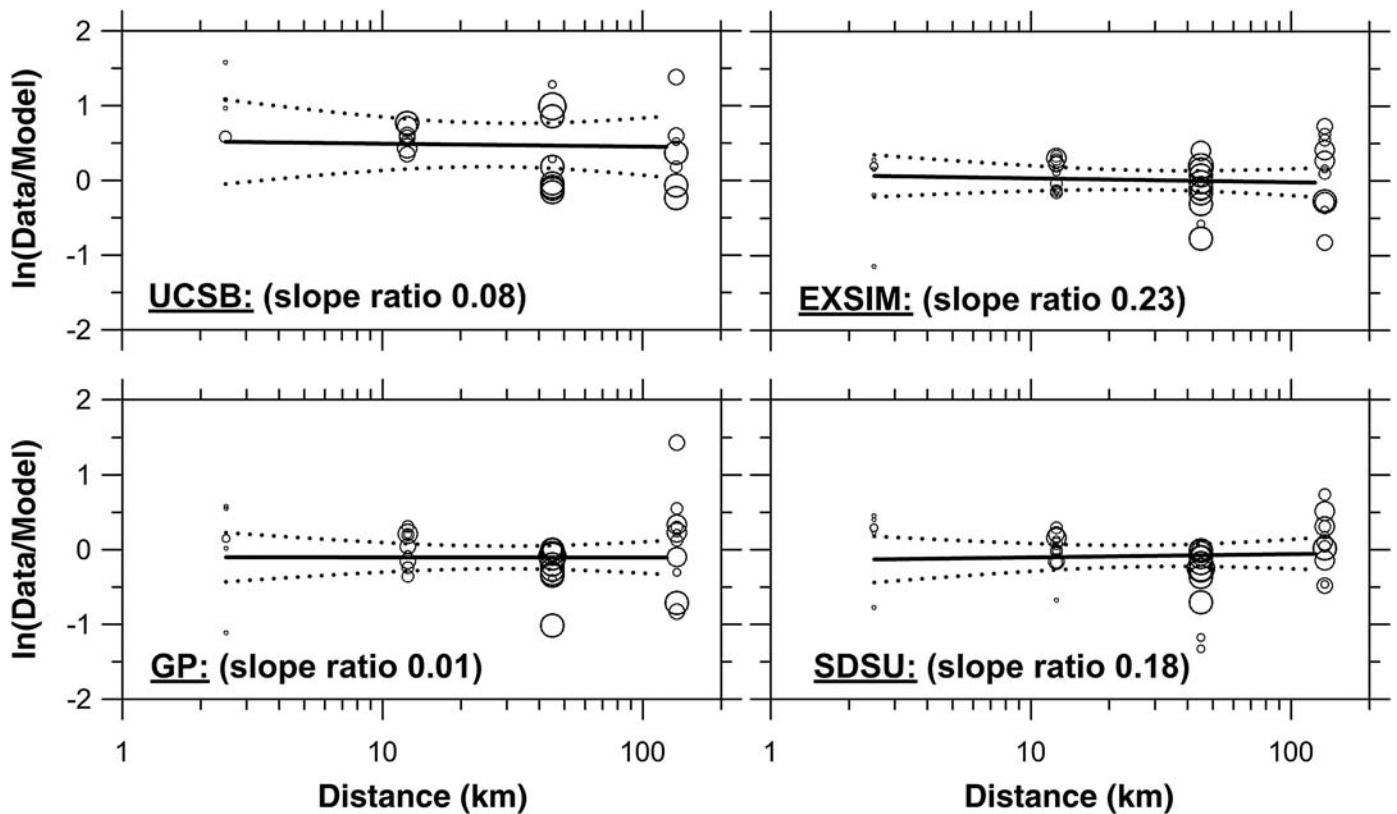
▲ **Figure 1.** Comparison of combined goodness of fit. The “Within Threshold” (white) threshold is 0.35 natural log units, and the “Problematic” (dark gray) threshold is 0.7 natural log units. Stippled indicates simulations that were not performed due to limited observations. The goodness of fit is classified by period and distance ranges.

Combined Metric Vs. GMPE																	
Better than GMPE Comparable to GMPE Inferior to GMPE																	
		0.01 ≤ PSA Period Range ≤ 0.1 s				0.1 < PSA Period Range ≤ 1 s				1 < PSA Period Range ≤ 3 s				PSA > 3s			
Event (M _w , Mech.)		UCSB	EXSIM	G&P	SDSU	UCSB	EXSIM	G&P	SDSU	UCSB	EXSIM	G&P	SDSU	UCSB	EXSIM	G&P	SDSU
R _{rup} =[0-5] km	Chino Hills (5.39, ROBL)																
	Alum Rock (5.45, SS)		0.78	0.71	0.49		0.86	0.83	0.59		0.65	0.75	0.75		0.58	0.67	0.63
	Whittier Narrows (5.89, REV)																
	North Palm Springs (6.12, ROBL)	1.53	2.38	0.78	2.25	6.19	1.48	0.71	1.74	6.20	1.33	3.10	3.40	0.82	0.16	1.88	1.90
	Tottori (6.59, SS)	0.85	5.13	0.57	1.7	1.74	0.66	0.95	0.73	11.9	1.81	1.33	1.6	2.71	0.56	0.73	0.76
	Niigata (6.65, REV)																
	Northridge (6.73, REV)																
	Loma Prieta (6.94, ROBL)	1.08	1.14	0.72	1.04	2.83	1.39	1.22	1.61	1.30	1.24	0.51	0.56	1.41	1.10	1.28	1.28
	Landers (7.22, SS)	1.10	0.70	0.87	0.88	2.29	0.41	0.80	0.65	2.17	0.65	0.62	0.56	1.92	0.97	0.38	0.38
	Riviere-du-Loup (4.6 REV)																
	Mineral (5.68 REV)																
	Saguenay (5.81 REV)																
	Average CA	1.29	0.96	0.77	0.99	2.53	0.72	0.74	0.84	2.28	1.08	0.98	1.02	2.60	1.20	0.90	0.88
Average CENA																	
Average ALL	1.25	1.20	0.82	0.97	3.03	0.92	0.97	1.03	2.68	1.06	1.00	1.06	2.66	1.00	0.88	0.86	
R _{rup} =[5-20] km	Chino Hills (5.39, ROBL)		0.59	0.38	0.50		1.48	1.19	1.29		4.27	4.87	4.33		2.96	2.96	3.11
	Alum Rock (5.45, SS)		0.66	1.09	0.40		0.86	1.31	0.63		1.12	1.24	1.28		1.64	1.00	0.99
	Whittier Narrows (5.89, REV)	1.36	0.93	1.20	1.20	3.71	1.54	1.32	1.37	1.05	0.48	1.07	1.24	0.25	0.45	1.26	1.25
	North Palm Springs (6.12, ROBL)	1.96	0.94	1.27	0.90	2.27	0.95	1.16	1.04	1.65	0.67	1.06	1.22	0.69	0.64	0.32	0.32
	Tottori (6.59, SS)	0.64	0.78	0.59	0.51	0.73	0.34	0.66	0.39	2.14	0.93	1.23	1.14	2.51	1.70	1.14	1.12
	Niigata (6.65, REV)	0.91	0.72	0.76	0.71	1.46	0.93	0.76	0.54	0.38	0.73	1.35	1.44	0.43	0.56	0.99	1.01
	Northridge (6.73, REV)	2.71	1.49	0.98	1.05	2.48	1.17	1.00	0.91	1.50	1.07	0.61	0.68	1.30	1.26	0.74	0.74
	Loma Prieta (6.94, ROBL)	0.81	1.52	0.83	1.10	1.74	1.13	0.76	1.09	2.10	1.23	1.77	1.85	2.04	1.47	1.18	1.18
	Landers (7.22, SS)	2.25	1.32	1.38	1.46	1.97	0.97	0.80	0.85	2.39	1.93	1.86	1.98	1.05	0.98	2.02	2.02
	Riviere-du-Loup (4.6 REV)		1.07	0.41	0.32		1.00	1.15	1.12		1.92	1.97	1.83		1.31	1.29	1.38
	Mineral (5.68 REV)	1.04	0.65	0.61	0.93	1.86	0.56	0.75	1.92	2.88	0.63	0.16	0.72	3.00	1.47	0.16	1.32
	Saguenay (5.81 REV)																
	Average CA	1.13	0.96	0.96	0.80	3.00	1.27	0.98	1.02	0.50	0.27	0.32	0.35	1.48	1.67	1.13	1.12
Average CENA	1.18	0.91	0.48	0.55	1.50	0.91	1.18	1.31	0.92	0.59	0.54	0.48	0.81	1.33	1.20	1.29	
Average ALL	1.24	1.02	1.00	1.04	2.30	1.02	0.84	0.84	0.48	0.27	0.33	0.36	1.44	1.54	1.24	1.26	
R _{rup} =[20-70] km	Chino Hills (5.39, ROBL)		0.79	0.52	0.48		0.78	0.67	0.63		1.90	1.44	1.19		2.29	2.16	2.11
	Alum Rock (5.45, SS)		0.76	1.03	0.76		0.96	1.23	0.89		0.71	0.93	0.95		0.52	1.33	1.35
	Whittier Narrows (5.89, REV)	1.39	1.31	0.84	1.15	3.69	1.30	1.02	1.41	1.52	0.57	0.90	1.09	1.21	0.46	1.51	1.61
	North Palm Springs (6.12, ROBL)	0.83	1.46	1.07	0.98	3.09	1.07	0.88	0.88	2.10	1.09	0.58	0.70	1.56	3.78	4.78	4.78
	Tottori (6.59, SS)	0.19	0.29	0.72	0.34	0.66	0.64	0.62	0.58	0.78	1.02	1.30	1.36	0.96	0.54	1.40	1.40
	Niigata (6.65, REV)	0.75	0.65	0.80	0.49	1.20	0.88	1.32	1.00	0.77	0.78	1.49	1.52	1.28	0.56	1.54	1.54
	Northridge (6.73, REV)	1.68	0.63	0.95	1.73	1.08	1.17	1.42	1.73	0.77	1.51	0.93	1.00	1.60	1.30	2.13	2.13
	Loma Prieta (6.94, ROBL)	1.74	0.74	1.46	1.12	1.06	1.13	1.81	1.28	0.96	1.52	2.06	2.13	1.01	0.81	0.56	0.56
	Landers (7.22, SS)	3.53	0.83	1.36	1.17	1.43	1.40	1.43	1.34	0.97	1.47	1.26	1.31	0.84	1.08	1.95	1.95
	Riviere-du-Loup (4.6 REV)		0.38	0.38	0.29		1.25	0.67	0.80		0.55	0.39	0.45		0.39	0.36	0.38
	Mineral (5.68 REV)	0.17	0.49	0.26	0.17	1.21	0.84	1.45	3.16	1.23	1.32	0.95	0.72	0.63	1.99	0.07	0.13
	Saguenay (5.81 REV)	1.07	0.36	0.64	0.19	3.66	1.69	0.60	3.80	0.20	1.00	0.73	1.36				
	Average CA	1.11	0.67	1.00	0.95	1.52	0.89	1.18	1.10	0.86	1.00	1.03	1.11	1.30	1.06	1.94	1.94
Average CENA	0.82	0.39	0.41	0.24	2.14	1.11	0.70	1.35	1.11	0.68	0.43	0.52	0.68	0.64	0.36	0.40	
Average ALL	1.23	0.89	0.98	1.00	1.47	0.88	1.18	1.15	0.61	0.88	1.06	1.13	1.10	0.65	1.58	1.58	
R _{rup} =[70-200 or 300] km	Chino Hills (5.39, ROBL)		1.65	1.57	1.32		1.39	1.48	1.47		1.38	1.57	1.46		1.37	1.58	1.57
	Alum Rock (5.45, SS)		0.77	0.80	0.66		1.00	0.99	0.70		0.75	2.31	2.38		0.74	4.10	4.10
	Whittier Narrows (5.89, REV)																
	North Palm Springs (6.12, ROBL)	1.04	0.61	0.35	1.00	1.22	1.07	0.84	1.13	2.36	1.30	1.06	0.84				
	Tottori (6.59, SS)	0.78	0.86	1.13	0.69	0.97	1.38	1.04	1.55	0.61	1.02	0.97	1.00	0.86	2.56	1.41	1.41
	Niigata (6.65, REV)	0.70	0.62	0.70	0.86	0.46	0.55	0.98	0.40	0.67	0.50	1.27	1.28	1.47	0.36	1.63	1.63
	Northridge (6.73, REV)	1.69	1.57	1.74	0.94	0.77	0.81	1.00	0.86	0.49	1.54	0.77	0.79	0.17	3.20	1.77	1.77
	Loma Prieta (6.94, ROBL)	0.53	1.36	0.91	1.20	0.86	0.87	0.79	1.03	0.79	0.74	0.62	0.60	0.84	0.62	0.41	0.41
	Landers (7.22, SS)	0.95	0.43	0.51	0.78	2.02	1.48	0.91	1.11	1.53	0.81	0.51	0.47	1.24	0.43	0.32	0.32
	Riviere-du-Loup (4.6 REV)		0.30	0.29	0.15		0.78	0.57	0.38		1.31	1.09	0.97		6.26	4.45	3.74
	Mineral (5.68 REV)	0.46	0.25	0.35	0.16	1.35	0.31	0.35	0.40	2.28	0.88	1.35	1.25	0.61	1.42	0.33	0.32
	Saguenay (5.81 REV)	1.52	0.29	0.62	0.12	2.43	0.52	0.97	0.20	4.34	0.78	2.43	0.84	2.54	0.46	1.42	0.50
	Average CA	0.46	0.77	0.69	0.70	1.38	1.06	0.91	0.84	1.79	0.78	0.87	0.91	1.71	0.72	0.64	0.64
Average CENA	1.13	0.27	0.41	0.13	2.22	0.50	0.72	0.29	3.55	0.99	1.87	1.13	0.71	1.44	0.39	0.33	
Average ALL	0.97	0.66	0.74	0.55	1.87	0.78	0.84	0.82	1.65	0.80	1.18	1.21	1.40	1.22	1.66	1.66	

▲ **Figure 2.** The combined metric goodness-of-fit numbers in Figure 1 are divided by the corresponding numbers for the ground-motion prediction equation (GMPE). White cells indicate a bias lower than the GMPE, and dark gray cells indicates a bias significantly larger than the GMPE. Stippled cells indicate scenarios that were not computed due to limited observations.

if a larger $\pm 0.5 \ln$ unit threshold is used for periods under 3 s and distances of 5–200 km. A tabulation for all of the simulation procedures and period ranges reveals that 62%, 90%, 80%, and 74% of the cells have CGOF < 0.70 for the four distance bins, respectively (i.e., a nonfailure condition), and 34%,

46%, 37%, and 35% of the cells have CGOF < 0.35 (pass condition). For the BBP as a whole, the methods perform better than a factor of 2 in simulating PSAs for a large majority of the different earthquake, period, and distance test cases. At longer periods, all of the methods tend to show increases in bias,



▲ **Figure 3.** Comparison of mean bias from $\text{\textcircled{E}}$ Figure S1 for the four discrete distance bins (circles) for the four simulation methods evaluated in v14.3. The results shown are for pseudospectral acceleration (PSA) in the 0.1–1.0 s oscillator period range. The fit line shows the least-squares fit to equation (1), and the dashed lines show the 95% confidence interval. The size of the symbols reflects the weight assigned in the least-squares fit, which depends on the number of points populating the bins for each event. The slope ratio is the ratio of the estimated slope and the 95% confidence of the estimate of the slope. A ratio less than 1 indicates that a slope of zero (no distance bias) is within the 95% confidence interval.

which could be due to simplifications of the velocity models used to compute Green’s functions, which are at this stage limited to 1D structures.

Pass Thresholds for Distance and Period Ranges Compared with GMPE

Normalizing the CGOF values in Figure 1 by the corresponding values for the GMPE can account for possible nonzero event terms, as well as provide an objective assessment of the simulations with respect to the GMPEs. The normalization is undertaken by dividing the simulation CGOF by the GMPE CGOF for each respective cell. Figure 2 shows the normalized CGOF values, where white cells indicate improved performance of a simulation relative to the GMPE (ratio < 1), and dark gray indicates significantly worse performance of a simulation than the GMPEs (ratio > 1.5). This scaling accounts for some of the event-specific problems seen in Figure 1, particularly for Alum Rock, Landers, and Rivière-du-Loup; however, these event-specific biases across methods are not completely eliminated. The selected GMPEs were not designed to be used for Japanese and CENA events, so they are provided as a baseline comparison only. A tabulation for all of the simulation methods and

period ranges in Figure 2 reveals that 71%, 76%, 79%, and 80% of the cells have normalized CGOF ≤ 1.5 for the four distance bins, respectively (i.e., a nonfailure condition), and 51%, 41%, 48%, and 58% of the cells have normalized CGOF ≤ 1.0 , indicating performance better than the GMPEs.

A tabulation of Figure 2 results for each method reveals that the UCSB, EXSIM, G&P, and SDSU methods perform better than GMPEs in 36%, 56%, 53%, and 49% of the cases and worse than GMPEs in 41%, 16%, 17%, and 21% of the cases. EXSIM, G&P, and SDSU have superior performance (70% of cases are better than the considered GMPEs) between 0.01 and 1 s and similarly good performance between 1 and 3 s. For periods greater than 3 s, EXSIM is noticeably better than the other simulation methods.

Distance Metric

One of the first-order effects that a simulation method should capture is the trend of ground motion with distance. Significant misfits in this behavior indicate calibration of the simulation method is required to better capture the effects of geometric spreading and anelastic attenuation. We assessed the ability of the simulation methods to correctly capture the

distance dependence of PSA in the part A validation by plotting the mean bias versus distance. This analysis uses mean residual bias for each bin (computed as $\ln[\text{data}/\text{model}]$, which can be positive or negative; \ominus Fig. S1), not the CGOF metric. Because there are 12 earthquakes, there are generally 12 values of mean bias to plot for each of four distance bins. We then fit a log-linear expression through the data points as follows:

$$\bar{R}(\bar{R}_{\text{rup}}) = a + b \times \ln(\bar{R}_{\text{rup}}), \quad (2)$$

in which \bar{R}_{rup} is the average site-source rupture distance for each distance bin range, a and b are regression coefficients, and \bar{R} is the distance-dependent average of the mean residuals. Coefficients are determined using a weighted least-squares fit in which each datum is weighted by the number of periods and stations in each bin for each event. Confidence intervals (95%) on the mean trend line are computed. Examples of these plots for each simulation method are shown in Figure 3.

A general characteristic of all methods examined in this way is that the dispersion of mean bias increases with increasing distance. This is likely due to the increasing effects of lateral heterogeneity for the longer paths in the data and to large surface waves that propagate to great distances due to the lack of scattering in the shallow continuous layers of the 1D velocity models.

The performance of the simulation methods with respect to distance can be judged from the slope of the trend lines in Figure 3 (i.e., parameter b). We consider a method as passing this criterion if the zero slope falls within the 95% confidence interval on b . We define b_{95} as the two-tailed Student's t 95% confidence interval range on b . Table 1 shows the resulting $\text{abs}(b_{\text{sims}})$ divided by b_{95} . Values of this ratio less than 1 indicate that zero slope ($b = 0$) lies within the 95% confidence interval, which constitutes a passing condition (nonitalicized data). The failure threshold is set for ratios above 1, and the corresponding cell is italicized. The ratios for each period bin are summarized in Table 1. Although earlier versions of the BBP simulation methods did not pass this criterion (Dreger *et al.*, 2013), the four v14.3 models perform well.

PART B VALIDATION COMPARISON WITH PUBLISHED GMPE

In the part B validation, we compared mean $\ln(\text{PSA})$ from simulations and GMPEs for M 5.5 (reverse), 6.2 (strike-slip), and 6.6 (reverse and strike-slip) events at distances of 20 and 50 km for the 0.01–3 s period range. These cases were used because there are many observed data for those magnitudes and distances, and as a result, the GMPEs are well constrained. For each magnitude, a couple sets of 50 source realizations and hypocenter locations are considered. The simulation methods that are deterministic or have a deterministic component used Green's functions for two different velocity models for southern and northern California. Both strike-slip and reverse-slip cases were considered. Only footwall motions were considered for the reverse-slip cases.

Table 1
Distance Metric

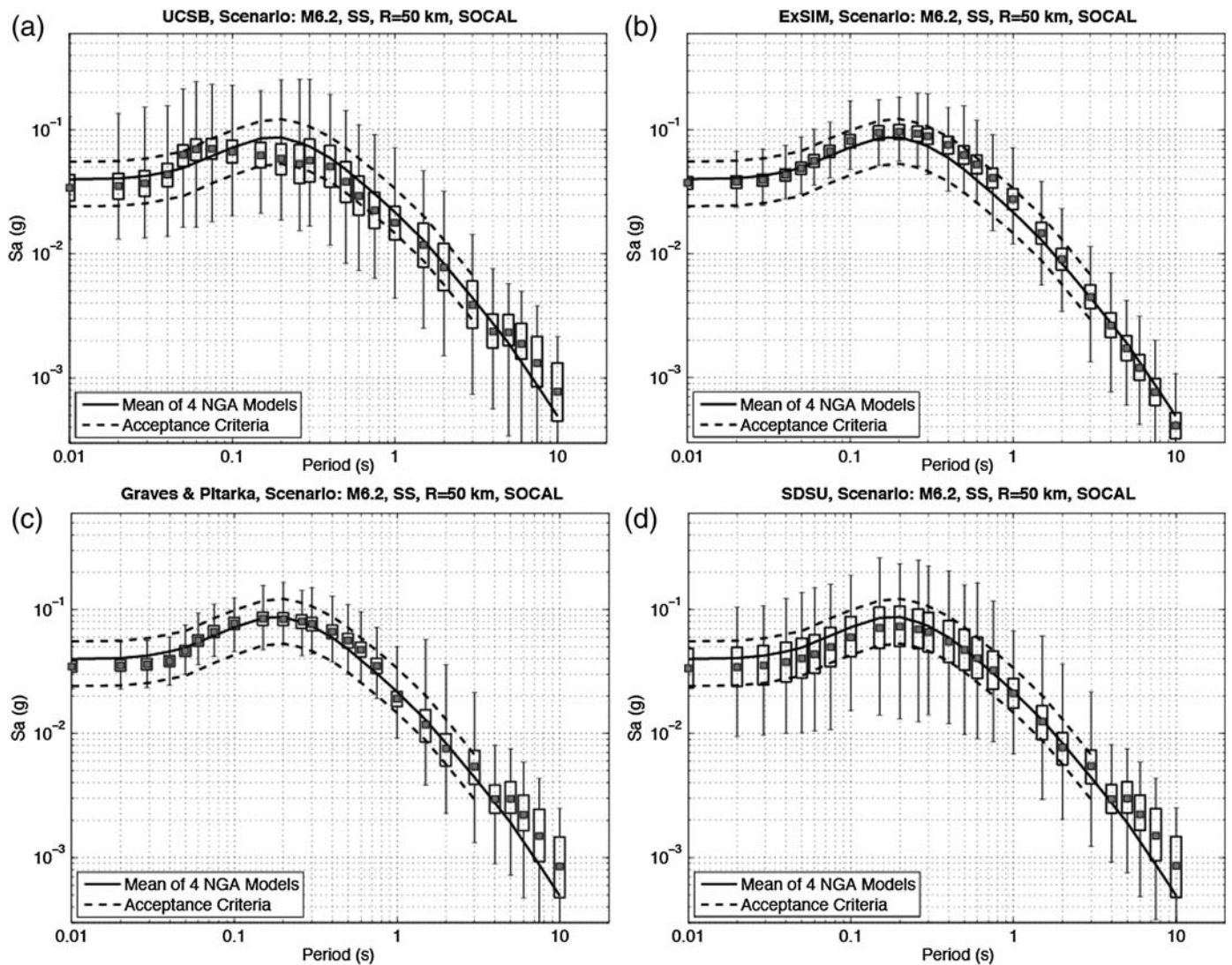
Period (s)	Simulation Method				
	UCSB	EXSIM	G&P	SDSU	GMPE
0.01–0.1	0.38	0.36	0.67	0.57	0.53
0.1–1	0.08	0.23	0.01	0.18	0.03
1–3	0.16	0.10	0.05	0.04	0.11
>3	1.19	0.34	0.83	0.87	0.13

Figure 4 shows an example of such a comparison of the simulated ground motions for the UCSB, EXSIM, G&P, and SDSU methods for an M 6.2 strike-slip event at a distance of 50 km for a southern California velocity model (SOCAL) case. The mean of the 50 source realizations is shown as the square, the standard deviation as the box, and the minimum and maximum extremes of all realizations are shown with the bars. In each plot, the median ground motion obtained from the four NGA-West 1 GMPEs (i.e., the median of the medians from individual models) is shown as a thick black line.

Since at the start of the validation only the NGA-West 1 models had been published, the centering criterion was based on the median of those models (solid line in Fig. 4). The acceptance criteria (dashed lines), as described in Goulet *et al.* (2015), were derived from the spread of preliminary models of the NGA-West 2 GMPE medians that became available during the validation (see Bozorgnia *et al.*, 2014) by taking the largest absolute value of positive and negative departures of any individual GMPE median from the overall median (solid line) for any period under 3 s, adding 15%, and then applying that difference uniformly for all periods in the 0–3 s range. The effective range of the acceptance criteria corresponds to a range of about ± 1.46 ($\pm 0.38 \ln$ units). Because the criteria were defined in terms of the extreme excursions from the median at any period, but applied equally over all periods, they span a generously wide range. If a simulation median falls outside that range it is indicative of a significant departure from the recorded data set. Periods longer than 3 s are not considered because the GMPEs are less well constrained by data. The passing criterion is that the simulation median must lie within the acceptance criteria for all periods. All of the methods except for EXSIM produce PSAs larger than the GMPE means for periods > 3 s, although these differences appear to be magnitude dependent (smaller magnitudes showing better agreement).

DISCUSSION AND CONCLUSIONS

Objective validation of the BBP codes for finite-fault simulations of ground-motion PSA has been facilitated by the controlled computational environment of the BBP, its strict version control third-party (nondeveloper) operation for applications and testing, and its array of graphical and numerical output products (e.g., Maechling *et al.*, 2015; Goulet *et al.*, 2015). In this stage



▲ **Figure 4.** Comparison of the four (a) UCSB, (b) EXSIM, (c) G&P, and (d) SDSU PSA for an **M** 6.2, strike-slip scenario at a distance of 50 km. The solid squares show the mean motion, the boxes show the standard deviation, and the error bars show the maximum range of simulated motions for 50 source realizations. The black line shows the mean from four NGA-West 1 GMPEs, and the dashed curves are the acceptance limits of the mean motions as described in the text. SOCAL refers to the velocity model used by the G&P, SDSU, and UCSB simulation methods.

of the BBP development effort, the objective was to validate capabilities for simulating the median PSA of ground motions. The results from the part A and part B validations indicate that, under the criteria of this panel's evaluation, the UCSB, EXSIM, G&P, and SDSU methods can provide acceptable estimates of median PSA from 0.01 to 3 s oscillator period within the validation magnitude range (**M** 5.4–7.2) for earthquakes in California or in comparable active crustal regions. The available data are too limited to claim the methods are adequately validated for stable continental regions (i.e., CENA). For both tectonic environments (active crustal and stable continental), it is the opinion of the panel that the simulations can be used to provide insights into relative effects, or scaling relationships, that are unresolvable from data alone. For example, in active regions, this may include


analysis of changes in ground motion due to changes in source geometry, rupture direction, presence of secondary slip on splays, and hanging-wall effects. In stable continental regions, the recommendation is to use simulations for the development of fundamental within-method scaling relationships only (with magnitude and distance). Regardless of region, these relative effects are best utilized in combination with base case motions not derived solely from simulations (e.g., from a semi-empirical GMPE).

For periods above 1 s, there is increased bias relative to recordings, and above 3 s period there are significant deviations from GMPEs. This indicates the simulation methods are relatively accurate for short periods, where simulation method developers can tune the kinematic description of the source

and, in the case of the G&P and SDSU methods, the stochastic approach used for high frequencies. However, it is notable that the simulations are considerably less accurate at longer periods than the GMPEs (e.g., where the physics-based modeling should, in principal, provide the best results). Further analysis will be required to understand the source of this additional bias, but possible contributors include the specifics of the moment–area scaling relationships used in source generation for the simulations and unrealistic propagation efficiency of surface waves from the employed 1D velocity models. In addition, above 3 s period the uncertainties in the GMPE medians themselves, in some cases, may be comparable to the differences between the simulations and GMPEs. Future work should investigate systematic differences in simulated motions from 1D versus 3D velocity structures and repeat the part B validations using the final NGA-West 2 models, which are more reliable than the NGA-West 1 models at periods beyond 3 s (e.g., Bozorgnia *et al.*, 2014). In addition, we have validated neither the polarizations of the 1D simulated ground motions nor their numerical accuracy at sites within a few kilometers of a surface-rupturing event, where numerical accuracy is difficult to achieve (e.g., Hisada and Bielak, 2003).

It should be recognized that when the simulations are applied at magnitudes beyond the validation range, the results have additional epistemic uncertainty that has not been formally investigated. Although formal validations of the methods are not currently possible for $M > 8$, their use at higher magnitude will require better understanding of epistemic uncertainties related to various model assumptions and inputs, including scaling and effects of stress parameters (stochastic approaches), subfault stress drop (deterministic approaches), parameterization of slip velocity function, and the frequency of occurrence of super-shear rupture velocity in earthquakes having $M > 7.2$.

In future validations of the BBP, several other measures of goodness-of-fit should be considered. The specific metrics would depend on the desired engineering application but could include (1) inelastic PSA, (2) time of the maximum oscillator response and other peak ground motion parameters, (3) limit of static offset in displacement time series as a function of distance from fault, (4) measures that assess the spectral shape of PSA and Fourier amplitude spectra (e.g., adherence to $1/f^2$), (5) duration, and (6) other quantified time-domain features of strong motions. Some of these will be important for engineering applications that directly use time series.

This article summarized the validation of simulation methods implemented on v14.3 of the BBP, essentially providing a snapshot in time. The validation process is still ongoing, and we expect to foster further refinement of existing methods and the implementation of new methods as we continue the validation against additional scenarios. 

ACKNOWLEDGMENTS

We thank Tran Huynh, Fabio Silva, and Phil Maechling for their administrative and information technology support

and Paul Somerville for technical and scientific management. We thank the simulation modelers for their cooperation: Gail Atkinson, John Anderson, Ralph Archuleta, Karen Assatourians, Jorge Crempien, Robert Graves, Kim Olsen, Arben Pitarka, Rumi Takedatsu, and Jeff Bayless. Carola Di Alessandro and David Boore provided SMSIM results for comparison with the BBP results. This research was supported by the Southern California Earthquake Center (SCEC). SCEC is funded by National Science Foundation Cooperative Agreement EAR-1033462 and U. S. Geological Survey Cooperative Agreement G12AC20038. The SCEC contribution number for this article is 1983. We acknowledge the Pacific Earthquake Engineering Research (PEER) Center for providing the recorded data and for supporting Christine Goulet in her leadership role with the group.

REFERENCES

- Abrahamson, N. A., and W. J. Silva (2008). Summary of the Abrahamson and Silva NGA ground motion relations, *Earthq. Spectra* **24**, no. S1, 67–97.
- Anderson, J. (2015). The composite source model for broadband simulations of strong ground motions, *Seismol. Res. Lett.* **86**, no. 1, doi: [10.1785/0220140098](https://doi.org/10.1785/0220140098).
- Atkinson, G. M., and K. Assatourians (2015). Implementation and validation of EXSIM (a stochastic finite-fault ground-motion simulation algorithm), *Seismol. Res. Lett.* **86**, no. 1, doi: [10.1785/0220140097](https://doi.org/10.1785/0220140097).
- Boore, D. M. (2010). Orientation-independent, nongeometric-mean measures of seismic intensity from two horizontal components of motion, *Bull. Seismol. Soc. Am.* **100**, 1830–1835.
- Boore, D. M., and G. M. Atkinson (2008). Ground motion prediction equations for the average horizontal component of PGA, PGV, and 5%-damped PSA at spectral periods between 0.01 and 10.0 s, *Earthq. Spectra* **24**, no. S1, 99–138.
- Bozorgnia, Y., N. A. Abrahamson, L. Al Atik, T. D. Ancheta, G. M. Atkinson, J. W. Baker, A. Baltay, D. M. Boore, K. W. Campbell, B. S.-J. Chiou, R. Darragh, S. Day, J. Donahue, R. W. Graves, N. Gregor, T. Hanks, I. M. Idriss, R. Kamai, T. Kishida, A. Kottke, S. A. Mahin, S. Rezaeian, B. Rowshandel, E. Seyhan, S. Shahi, J. P. Stewart, J. Watson-Lamprey, K. Wooddell, and R. Youngs (2014). NGA-West2 research project, *Earthq. Spectra* **30**, no. 3, 973–987.
- Campbell, K. W., and Y. Bozorgnia (2008). NGA ground motion model for the geometric mean horizontal component of PGA, PGV, PGD, and 5%-damped linear elastic response spectra for periods ranging from 0.01 to 10 s, *Earthq. Spectra* **24**, no. S1, 139–171.
- Chiou, B. S.-J., and R. R. Youngs (2008). An NGA model for the average horizontal component of peak ground motion and response spectra, *Earthq. Spectra* **24**, no. S1, 173–215.
- Crempien, J., and R. Archuleta (2015). UCSB method for broadband ground motion from kinematic simulations of earthquakes, *Seismol. Res. Lett.* **86**, no. 1, doi: [10.1785/0220140103](https://doi.org/10.1785/0220140103).
- Dreger, D. S., G. C. Beroza, S. M. Day, C. A. Goulet, T. H. Jordan, P. A. Spudich, and J. P. Stewart (2013). Evaluation of SCEC Broadband Platform Phase 1 Ground Motion Simulation Results, *SCEC Report*, 2 August 2013, 33 pp., http://scec.usc.edu/scecpedia/SCEC_BB_PPhase_1_Evaluation (last accessed November 2014).
- Goulet, C. A., N. A. Abrahamson, P. G. Somerville, and K. E. Wooddell (2015). The SCEC Broadband Platform validation exercise: Methodology for code validation in the context of seismic hazard analyses, *Seismol. Res. Lett.* **86**, no. 1, doi: [10.1785/0220140104](https://doi.org/10.1785/0220140104).

- Graves, R., and A. Pitarka (2015). Refinements to the Graves and Pitarka (2010) broadband ground motion simulation method, *Seismol. Res. Lett.* **86**, no. 1, doi: [10.1785/0220140101](https://doi.org/10.1785/0220140101).
- Hisada, Y., and J. Bielak (2003). A theoretical method for computing near-fault ground motions in layered half-spaces considering static offset due to surface faulting, with a physical interpretation of fling step and rupture directivity, *Bull. Seismol. Soc. Am.* **93**, no. 3, 1154–1168.
- Maechling, P. J., F. Silva, S. Callaghan, and T. H. Jordan (2015). SCEC broadband platform: System architecture and software implementation, *Seismol. Res. Lett.* **86**, no. 1, doi: [10.1785/0220140125](https://doi.org/10.1785/0220140125).
- Olsen, K., and R. Takedatsu (2015). The SDSU broadband ground motion generation module BBtoolbox Version 1.5, *Seismol. Res. Lett.* **86**, no. 1, doi: [10.1785/0220140102](https://doi.org/10.1785/0220140102).
- Star, L. M., J. P. Stewart, and R. W. Graves (2011). Comparison of ground motions from hybrid simulations to NGA prediction equations, *Earthq. Spectra* **27**, no. 2, 331–350.

Douglas S. Dreger
Department of Earth and Planetary Science
281 McCone Hall
University of California Berkeley
Berkeley, California 94720 U.S.A.
dreger@seismo.berkeley.edu

Gregory C. Beroza
School of Earth Sciences
Mitchell 355
Stanford University
Stanford, California 94305 U.S.A.
beroza@stanford.edu

Steven M. Day
Department of Geological Sciences
5500 Campanile Drive

San Diego State University
San Diego, California 92115 U.S.A.
sday@mail.sdsu.edu

Christine A. Goulet
Pacific Earthquake Engineering Research Center
325 Davis Hall
University of California Berkeley
Berkeley, California 94720 U.S.A.
goulet@berkeley.edu

Thomas H. Jordan
Department of Earth Sciences
Zumberge Hall of Science
University of Southern California
Los Angeles, California 90089 U.S.A.
tjordan@usc.edu

Paul A. Spudich
U.S. Geologic Survey
345 Middlefield Road
Menlo Park, California 94025 U.S.A.
spudich@usgs.gov

Jonathan P. Stewart
Department of Civil and Environmental Engineering
5731 Boelter Hall
University of California Los Angeles
Santa Monica, California 90095 U.S.A.
jstewart@seas.ucla.edu

Published Online 17 December 2014